Journal of the Physical Society of Japan
Vol. 68, No. 5, May, 1999, pp. 1492-1495

Electron-Electron Umklapp Process in Two-Dimensional Electron Gas under a Spatially Alternating Magnetic Field

Mayumi KATO, Akira ENDO, Makoto SAKAIRI, Shingo KATSUMOTO* and Yasuhiro IYE*

Institute for Solid State Physics, University of Tokyo, Roppongi, Minato-ku, Tokyo 106-8666

(Received January 14, 1999)

We have studied the transport phenomenon in two-dimensional electron gas at a GaAs/AlGaAs heterointerface placed in a spatially alternating magnetic field. The effect of the periodic magnetic field is twofold. One is the effective mass renormalization which manifests itself as resistivity enhancement in the $T \to 0$ limit. The other is a T^2-dependent relaxation rate which is attributed to the electron-electron Umklapp scattering. A similar phenomenon observed at higher bias current provides additional support to this interpretation and forms a basis for a new method of hot electron thermometry.

KEYWORDS: electron-electron scattering, Umklapp process, 2DEG, GaAs/AlGaAs, hot electron

Although the electron-electron interaction is inarguably one of the most essential processes in condensed matter physics, its role in transport phenomena is rather subtle. It plays an important role in establishing a thermal equilibrium among electrons and in affecting their phase coherence. It cannot, however, contribute to resistivity in a Galilean invariant system having continuous translational symmetry, because the total momentum of two colliding electrons is conserved there. It is only with the participation of a crystal lattice, i.e. the Umklapp process, that momentum relaxation occurs by electron-electron scattering.[1] When it does occur, the electron-electron Umklapp scattering gives rise to a T^2-dependent resistivity. Such a T^2-term in resistivity is conspicuous in strongly correlated electron systems such as heavy fermion metals, transition metal oxides and organic conductors. Although there has been much progress in the theoretical understanding of the issue,[2-4] a truly quantitative comparison between theory and experiment seems difficult at the moment, because a full treatment of the relevant electron-electron process involves details of the complex band structure of real materials. It is desirable, thus, to find the simplest possible experimental system that exhibits the phenomenon at issue.

In our recent publication,[5] we reported that the effect of electron-electron Umklapp scattering can be observed in a two-dimensional electron gas (2DEG) at a $GaAs/Ga_{1-x}Al_xAs$ heterointerface by imposing an artificial superperiodicity in the form of a spatially alternating magnetic field $B_z(x) = B_0 \cos(Kx)$ normal to the 2DEG plane. It has been found that the excess resistivity varies as $\Delta\rho = AT^2 + C$, and is proportional to the square of the amplitude B_0 of the magnetostatic modulation. This is a unique case in which the contribution of electron-electron scattering to resistivity can be externally controlled by an artificially imposed superperiodicity. Similar observation was reported by Overend *et al.*[6]

In this letter, based on the observation of the anisotropic manifestation of the effect, we argue that the magnetostatic lateral superlattice gives rise to not only extra scattering proportional to T^2, which is attributable to the electron-electron process, but also to renormalization of the effective mass. We also investigated the effect of increased current bias and found a similar effect with T substituted with the electron temperature T_e. This result furnishes a strong piece of evidence in support of the above picture, and forms the basis of a new method of hot electron thermometry.

We should point out that it is also possible to investigate the effect using a more conventional electrostatic modulation, as pioneered by Messica *et al.*[7] The use of magnetostatic modulation as employed here, however, has distinct advantages in some respects. First, it allows us to vary the modulation amplitude without affecting the electron density which should be kept constant when we attempt to investigate the effects of electron-electron interaction. Second, the spatial profile of magnetostatic modulation can be calculated straightforwardly, while that of electrostatic modulation requires sophisticated calculations taking into account the screening effect.

The samples used in the present study were fabricated from a $GaAs/Ga_{1-x}Al_xAs$ single heterojunction wafer with electron density $n_e \approx 3 \times 10^{15}\,\mathrm{m}^{-2}$ and mobility $\mu \approx 60\,\mathrm{m}^2/\mathrm{Vs}$ at 4.2 K. The depth of the heterointerface from the top surface was 75 nm. A Hall bar pattern was defined by standard photolithography and wet chemical etching with the current path oriented parallel to the $\langle 100 \rangle$ direction. A stripe-patterned ferromagnetic gate electrode was then fabricated on the surface by electron beam lithography, deposition of a 60 nm thick cobalt film by ion beam sputtering and lift-off. The periodicity of the stripe-pattern was $a = 2\pi/K = 500$ nm, and each stripe was 250 nm wide. The reason for the choice of the crystalline orientation $\langle 100 \rangle$ is to minimize the influ-

* Also at CREST, Japan Science and Technology Corporation, Mejiro, Toshima-ku, Tokyo 171-0031.

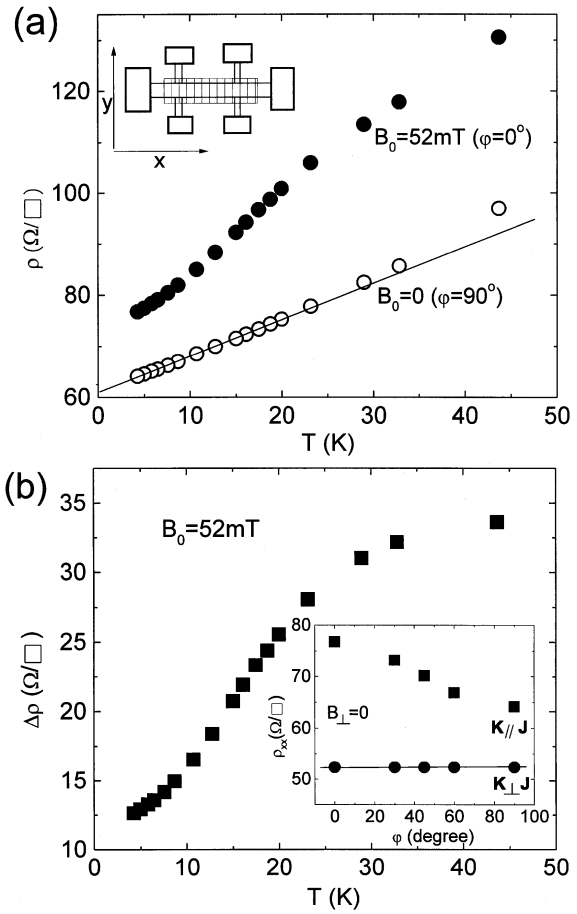

Fig. 1. (a) The inset shows the structure of the sample with the modulation wave vector parallel to the current channel. The main panel shows the temperature dependence of resistivity under maximum magnetic modulation ($\varphi = 0°$: solid circles) and no modulation ($\varphi = 90°$: open circles). (b) Temperature dependence of the excess resistivity $\Delta\rho$. The inset shows comparison of the effect of magnetostatic modulation on resistivity between the ($\mathbf{K} \parallel \mathbf{J}$) sample and the ($\mathbf{K} \perp \mathbf{J}$) sample at $T = 1.3\,\mathrm{K}$.

ence of the strain-induced electrostatic potential modulation.[8,5] In the samples for principal studies, the stripe pattern was fabricated with the modulation wave vector $\mathbf{K}$ parallel to the current channel, as illustrated in the inset of Fig. 1(a). For control experiments, another types of samples with $\mathbf{K}$ perpendicular to the current channel were prepared. In this paper, these two types of samples will be identified as $\mathbf{K} \parallel \mathbf{J}$ and $\mathbf{K} \perp \mathbf{J}$, respectively.

Resistance measurements were carried out by a standard low-frequency a.c. four probe method. A cross-coil magnet system consisting of a 6 T split-coil superconducting magnet and a small homemade solenoid, enabled us to control the horizontal and vertical components of the magnetic field independently. A rotating sample holder was used to align the 2DEG plane to the horizontal field within a few tenths of a degree. The vertical magnetic field was then swept so as to locate the point of exact alignment. When the external magnetic field is exactly parallel to the 2DEG plane, the uniform component of the perpendicular field is null and only the spatially alternating component $B_0 \cos(Kx)$ is present.[9] The magnetic field modulation amplitude B_0 at the 2DEG plane can be evaluated by analyzing the Weiss oscillation pattern of the magnetoresistance,[10,11]

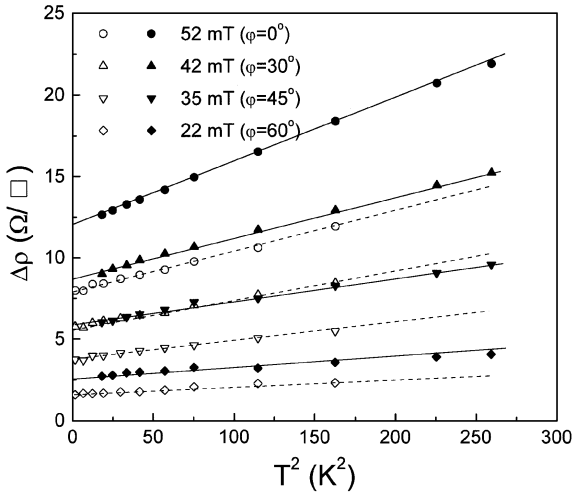

Fig. 2. $\Delta\rho$ plotted against T^2 for several values of modulation amplitude B_0, varied by changing φ. The solid and open symbols are the data taken from the same sample with different carrier densities, $n_\mathrm{e} = 2.9 \times 10^{15}\,\mathrm{m}^{-2}$ (dark) and $3.8 \times 10^{15}\,\mathrm{m}^{-2}$ (after illumination).

and it can be controlled by the azimuthal angle φ of the external field relative to the modulation wave vector $\mathbf{K}$.[5] The value of B_0 is maximum when $\mathbf{B} \parallel \mathbf{K}$, and zero when $\mathbf{B} \perp \mathbf{K}$. For the present samples with cobalt stripes, the maximum value was $B_0 = 52\,\mathrm{mT}$.

Let us first focus on the ($\mathbf{K} \parallel \mathbf{J}$) sample. Figure 1(a) shows the temperature dependence of resistivity for $\mathbf{B} \parallel \mathbf{K}$ ($B_0 = 52\,\mathrm{mT}$) and for $\mathbf{B} \perp \mathbf{K}$ ($B_0 = 0$). The resistivity for the latter case is basically the same as that of the plain 2DEG, and is written for $T < 40\,\mathrm{K}$ as

$$\rho_0(T) = \frac{1}{n_\mathrm{e} e}\left(\frac{1}{\mu_0} + \frac{1}{\mu_\mathrm{ph}(T)}\right)$$
$$\frac{1}{\mu_0} = \mathrm{const}, \quad \frac{1}{\mu_\mathrm{ph}(T)} = \alpha_\mathrm{ph} T. \qquad (1)$$

Here, $1/\mu_0$ is the temperature-independent inverse mobility limited by the elastic scattering due to impurities and $1/\mu_\mathrm{ph}$ is that limited by the acoustic phonon scattering rate which is T-linear in this temperature range.[12] Application of a spatially alternating magnetic field increases the resistivity by $\Delta\rho$. The temperature dependence of the excess resistivity $\Delta\rho \equiv \rho_{(\mathbf{B}\parallel\mathbf{K})} - \rho_{(\mathbf{B}\perp\mathbf{K})}$ is shown in Fig. 1(b).

Figure 2 shows the excess resistivity $\Delta\rho$ plotted against T^2 for several values of modulation amplitude B_0. These data were taken at several different settings of φ, which give different values of B_0, as mentioned above. Two sets of data in Fig. 2 at different carrier densities were taken from the same sample in the dark and after illumination. It is seen that $\Delta\rho$ at low temperatures ($T < 15\,\mathrm{K}$) can be expressed as $\Delta\rho = AT^2 + C$.

Similar measurements were carried out on a different sample with $\mathbf{K} \perp \mathbf{J}$. The solid circles in the inset of Fig. 1(b) indicate the total absence of the resistivity change in the ($\mathbf{K} \perp \mathbf{J}$) sample, while the solid squares show the $\cos^2\varphi$- (or, B_0^2-) dependence of $\Delta\rho$ in the ($\mathbf{K} \parallel \mathbf{J}$) sample.[13] The fact that the effect vanishes when the modulation wave vector is perpendicular to the

direction of transport current indicates that the effect is due to Umklapp backscattering by the periodic structure, and that a possible contribution from lithographical irregularity is of minor importance.

A strong piece of evidence that the excess resistivity is indeed due to electron-electron scattering, is obtained by a study of the hot electron effect. The measurement of excess resistivity similar to that described above was carried out as a function of bias current density with the sample kept at the lowest temperature (1.25 K). The electron temperature T_e for low to medium current bias was determined through the standard analysis of the Shubnikov-de Haas (SdH) oscillation amplitude. At a higher current bias, where SdH oscillations are no longer visible, we elected to use the following empirical relationship proposed by Hirakawa and Sakaki.[14)]

$$P_e = \beta_e (T_e^2 - T_L^2). \tag{2}$$

Here, T_L is the lattice temperature and P_e is the input power per electron. According to Hirakawa and Sakaki, the coefficient $\beta_e \approx 2.2 \times 10^{-16}\,\mathrm{W/K^2}$ is nearly independent of the electron density and mobility. We carried out the SdH measurements on the present sample and found that the above relationship holds, with a slightly different value of the coefficient, $\beta_e \approx 3.5 \times 10^{-16}\,\mathrm{W/K^2}$. We used this relationship to estimate T_e at higher values of bias current.

The inset of Fig. 3 shows the bias current dependence of the resistivity for the $\mathbf{B} \parallel \mathbf{K}$ (maximum modulation amplitude) and $\mathbf{B} \perp \mathbf{K}$ (modulation off) configurations. The current density independence of ρ for the latter case ensures that the lattice temperature remains unchanged even at the highest bias current. (A change in the lattice temperature would manifest itself as the T-linear resistivity due to acoustic phonon scattering.) The solid circles in the main panel of Fig. 3 show $\Delta\rho$ as a function of T_e^2. It is seen that they are in good agreement with the T^2-dependence (open triangles) taken at low current bias. This result furnishes an unmistakable piece of evidence that the observed resistivity increase is indeed due to the electron-electron scattering. We also note that the present result forms a basis for a possible new method of determining the temperature T_e of hot electrons. An advantage of this method over the more conventional method based on the Shubnikov-de Haas oscillation is that the former can be used at low (or even zero) magnetic fields and can be applied to low-mobility samples.

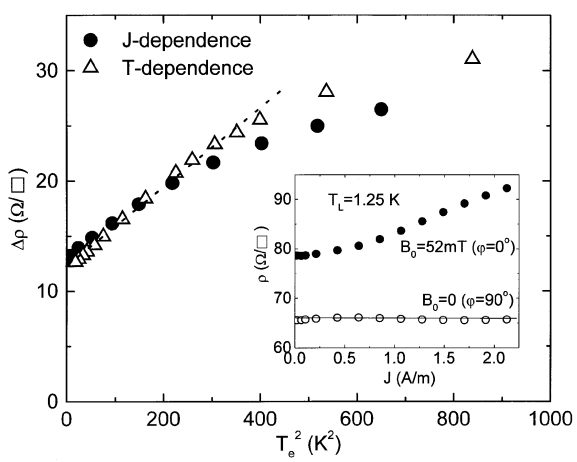

Fig. 3. The inset shows the current density dependence of the resistivity for the $\mathbf{B} \parallel \mathbf{K}$ (maximum modulation), and $\mathbf{B} \perp \mathbf{K}$ (modulation off) configurations. The main panel shows $\Delta\rho$ as a function of T_e^2 (solid circles) to be compared with the T^2-dependence in the low bias current limit (open triangles).

So far, we have concentrated on the T^2-term of the excess resistivity $\Delta\rho = AT^2 + C$. Now we turn to the term C, i.e., finite $\Delta\rho$ in the $T \to 0$ limit. In our previous paper,[5)] we interpreted it as a sort of "residual" term, which we tentatively attributed to some imperfection of the periodic structure. However, the total absence of the resistivity change for the ($\mathbf{K} \perp \mathbf{J}$) sample mentioned earlier makes such an interpretation highly unlikely. We thus re-interpret the finite $\Delta\rho$ in the $T = 0$ limit as an intrinsic effect associated with the superperiodicity, that is, a manifestation of effective mass renormalization.

The mechanism of effective mass renormalization in the presence of superperiodicity may be classified into two categories, the single-electron effect and the many-body effect. The former reflects a miniband formation due to Bragg reflection associated with the periodic structure, which leads to a dispersion $\varepsilon(\mathbf{k})$ altered from the original free-electron-like one.[15)] The latter, the many-body effect on the effective mass renormalization, is caused by the electron-electron Umklapp process.[4)] Although it is difficult at the moment to judge which of these mechanisms is more important in a particular case, the present system is a good candidate for experimental testground for theories since all the relevant parameters can be precisely determined.

Let us try to be more quantitative. The resistivity in the direction of the modulation wave vector may be written as

$$\rho(T) = \frac{1}{n_e e}\left(\frac{1}{\mu_0^*} + \frac{1}{\mu_{\mathrm{ph}}^*(T)} + \frac{1}{\mu_{\mathrm{ee}}(T)}\right),$$
$$\frac{1}{\mu_{\mathrm{ph}}^*(T)} = \alpha_{\mathrm{ph}}^* T, \quad \frac{1}{\mu_{\mathrm{ee}}(T)} = A_{\mathrm{ee}} T^2. \tag{3}$$

Here, $1/\mu_0^*$ and $1/\mu_{\mathrm{ph}}^*$ are the inverse mobilities associated with impurity scattering and phonon scattering, respectively. In general, a change in the effective mass affects the mobility $\mu^* = e\tau^*/m^*$, through m^* in the denominator and through a change in the scattering time τ^*. Figure 4 shows μ_0/μ_0^* and $A_{\mathrm{ee}} = \mu_{\mathrm{ee}}^{-1} T^{-2}$ extracted from the best fit of a functional form $\Delta\rho(T) = AT^2 + BT + C$. (As anticipated from Fig. 2, the T-linear term turns out to be very small.) These data for different carrier densities were taken from the same sample by making use of the persistent photoconductivity effect. Both μ_0/μ_0^* and A_{ee} are proportional to B_0^2, and the values for $B_0 = 52\,\mathrm{mT}$ are shown in Fig. 4.

The quantity μ_0/μ_0^* contains the effective mass enhancement factor m^*/m and the change in the scattering rate τ_0^*/τ_0. The mass dependence of the scattering rate is needed in order to disentangle the change in the effective mass and the change in the scattering rate. If the scattering rate is assumed unaffected by the presence of the

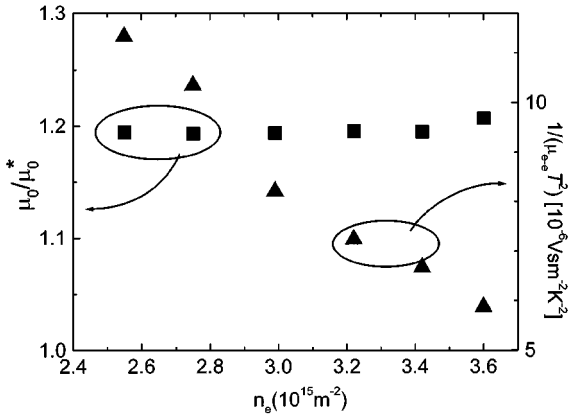

Fig. 4. μ_0/μ_0^* (squares) and $A_{ee} = \mu_{ee}^{-1}T^{-2}$ (triangles) for $B_0 = 52\,\mathrm{mT}$ as a function of the electron density n_e.

magnetostatic modulation, $\mu_0/\mu_0^* \sim 1.2$ for $B_0 = 52\,\mathrm{mT}$ is translated to an effective mass increase of 20%. On the other hand, if one assumes that the scattering rate changes according to $1/\tau_0 \propto m^{-1/2}$ for ionized impurity scattering, then $\mu_0/\mu_0^* = (m^*/m)^{1/2}$ so that the above value must be as large as 40%. These values seem to be too large because such a large change in the effective mass, if present, would also give rise to a significant change in the acoustic phonon scattering rate (T-linear term), which is not seen experimentally.

In Fig. 4, μ_0/μ_0^* is only weakly dependent on n_e. This is at odds with the expectation that the effective mass is sensitive to the position of the Fermi level in the subband structure. The n_e-dependence of A_{ee} is found to be $\sim n_e^{-1.9}$. This is steeper than the n_e^{-1}-dependence expected from $\tau_{ee}^{-1} \propto T^2/\varepsilon_F \propto n_e^{-1}$. Thus, although we believe that the effective mass renormalization effect due to the lateral magnetic superlattice is present, a quantitatively consistent model is yet to be constructed.

To summarize, we have investigated the resistivity increase in 2DEG caused by a spatially alternating magnetic field. The excess resistivity at finite temperatures shows a T^2-dependence characteristic of the electron-electron Umklapp process, which is brought into play by lifting of the Galilean invariance by the artificial lateral superlattice. The resistivity enhancement in the $T \to 0$ limit is taken as a manifestation of the effective mass renormalization due to miniband formation and/or the electron-electron Umklapp process. The present system is unique in that the relevant parameters are precisely known and can be externally controlled, so that comparison with theory can be performed unambiguously. We hope that it will serve as a prototype experimental system for the elucidation of electron-electron interaction in solids.

The authors thank Professor H. Fukuyama for his valuable comments. This work was supported in part by a Grant-in Aid for Scientific Research from the Ministry of Education, Science, Sports and Culture, Japan.

1) J. M. Ziman: *Electrons and Phonons* (Clarendon Press, Oxford, 1960).
2) K. Yamada and K. Yosida: Prog. Theor. Phys. **76** (1986) 621.
3) H. Maebashi and H. Fukuyama: J. Phys. Soc. Jpn. **66** (1997) 3577.
4) T. Okabe: J. Phys. Soc. Jpn. **67** (1998) 2792.
5) M. Kato, A. Endo and Y. Iye: Phys. Rev. B **58** (1998) 4876.
6) N. Overend, A. Nogaret, B. L. Gallagher, P. C. Main, R. Wirtz, R. Newbury, M. A. Howson and S. P. Beaumont: Physica B **249–251** (1998) 326.
7) A. Messica, A. Soibel, U. Meirav, A. Stern, H. Shtrikman, V. Umansky and D. Mahalu: Phys. Rev. Lett. **78** (1997) 705.
8) J. H. Davies and I. A. Larkin: Phys. Rev. B **49** (1994) 4800; I. A. Larkin, J. H. Davies, A. R. Long and R. Cusco: Phys. Rev. B **56** (1997) 15242; E. Skuras, A. R. Long, I. A. Larkin, J. H. Davies and M. C. Holland: Appl. Phys. Lett. **70** (1997) 871; A. Nogaret, S. Carlton, B. L. Gallagher, P. C. Main, M. Henini, R. Wirtz, R. Newbury, M. A. Howson and S. P. Beaumont: Phys. Rev. B **55** (1997) 16037.
9) Because of the small g-value of GaAs, the Zeeman effect due to the magnetic field parallel to the 2DEG plane can be ignored in the present field range.
10) F. M. Peeters and P. Vasilopoulos: Phys. Rev. B **47** (1993) 1466.
11) A. Endo, S. Izawa, S. Katsumoto and Y. Iye: Surf. Sci. **361/362** (1996) 333.
12) E. E. Mendez, P. J. Price and M. Heiblum: Appl. Phys. Lett. **45** (1984) 294; B. J. F. Lin, D. C. Tsui and G. Weimann: Solid State Commun. **56** (1985) 287.
13) Although the strain-induced electrostatic potential modulation due to the piezoelectric coupling is nullified by aligning the modulation vector to the ⟨100⟩ direction, one remains due to deformation potential coupling. The difference in the resistivity between the ($\mathbf{K} \parallel \mathbf{J}$) and ($\mathbf{K} \perp \mathbf{J}$) samples partly originates from this electrostatic potential modulation.
14) H. Hirakawa and H. Sakaki: Appl. Phys. Lett. **49** (1986) 889.
15) I. S. Ibrahim and F. M. Peeters: Phys. Rev. B **52** (1995) 17321; Am. J. Phys. **63** (1995) 171.